

Water Resources Research

RESEARCH ARTICLE

10.1002/2015WR018444

Key Points:

- Streamflow is reconstructed from an existing paleoclimate drought index
- Methodological innovation using rCCA addresses very high-dimensional data set
- Reconstructed streamflow provides insights into extreme, persistent high, and low flow

Supporting Information:

- Supporting Information S1

Correspondence to:

M. Ho,
mh3538@columbia.edu

Citation:

Ho, M., U. Lall, and E. R. Cook (2016),
Can a paleodrought record be used to reconstruct streamflow? A case study
for the Missouri River Basin, *Water
Resour. Res.*, 52, 5195–5212,
doi:10.1002/2015WR018444.

Received 1 DEC 2015

Accepted 7 JUN 2016

Accepted article online 9 JUN 2016

Published online 2 JUL 2016

Can a paleodrought record be used to reconstruct streamflow?: A case study for the Missouri River Basin

Michelle Ho¹, Upmanu Lall^{1,2}, and Edward R. Cook³

¹Earth Institute, Columbia Water Center, Columbia University, New York, New York, USA, ²Department of Earth and Environmental Engineering, Columbia University, New York, New York, USA, ³Lamont-Doherty Earth Observatory of Columbia University, Palisades, New York, USA

Abstract Recent advances in paleoclimatology have revealed dramatic long-term hydroclimatic variations that provide a context for limited historical records. A notable data set derived from a relatively dense network of paleoclimate proxy records in North America is the Living Blended Drought Atlas (LBDA): a gridded tree-ring-based reconstruction of summer Palmer Drought Severity Index. This index has been used to assess North American drought frequency, persistence, and spatial extent over the past two millennia. Here, we explore whether the LBDA can be used to reconstruct annual streamflow. Relative to streamflow reconstructions that use tree rings within the river basin of interest, the use of a gridded proxy poses a novel challenge. The gridded series have high spatial correlation, since they rely on tree rings over a common radius of influence. A novel algorithm for reconstructing streamflow using regularized canonical regression and inputs of local and global covariates is developed and applied over the Missouri River Basin, as a test case. Effectiveness in reconstruction is demonstrated with reconstructions showing periods where streamflow deficits may have been more severe than during recent droughts (e.g., the Civil War, Dust Bowl, and 1950s droughts). The maximum persistence of droughts and floods over the past 500 years far exceeds those observed in the instrumental record and periods of multidecadal variability in the 1500s and 1600s are detected. Challenges for an extension to a national streamflow reconstruction or applications using other gridded paleoclimate data sets such as adequate spatial coverage of streamflow and applicability of annual reconstructions are discussed.

1. Introduction

The concern with anthropogenic climate change and its hydrologic impacts has focused interest on how long-term climate variability may impact streamflow [e.g., Nohara *et al.*, 2006; Seager *et al.*, 2007]. The consequence of using short records to “over-allocate” the flows of major rivers are often cited as an example of the need for long records that can better inform the possible range of long-term variations of streamflow [Tootle and Piechota, 2006; McGowan *et al.*, 2009; Woodhouse *et al.*, 2010]. Continuous records of streamflow in the United States span several decades at best. Advances in paleoclimatology in the past few decades have provided opportunities across the world to extend the range of hydroclimatic variability [e.g., Quinn, 1992; Jones and Mann, 2004; Tierney *et al.*, 2010; Gallant and Gergis, 2011; Vance *et al.*, 2013; E. R. Cook *et al.*, 2013; Devineni *et al.*, 2013; Ho *et al.*, 2015]. While considerable uncertainty clouds the projections of hydroclimatic states towards the end of the 21st century, in the near to medium-term paleoclimate information may be crucial to inform the interannual to decadal variability of regional water availability as indicated by streamflow for reservoir operation, and agricultural and other water use decisions.

Paleoclimate reconstructions have been developed using proxies that typically span the past 1000–2000 years (also known as the Common Era). The North American region has a relatively dense network of high-resolution paleoclimate proxy records, primarily comprised of tree-ring chronologies. Tree-ring-proxy records have been used to assess various components of environmental variations [Fritts, 1976] including drought severity [e.g., Routson *et al.*, 2011; B. I. Cook *et al.*, 2015], pluvials [e.g., Woodhouse *et al.*, 2005; Peder-son *et al.*, 2012], streamflow variability [e.g., Woodhouse *et al.*, 2006; Prairie *et al.*, 2008; Allen *et al.*, 2013; Devineni *et al.*, 2013], and precipitation frequency [Woodhouse and Meko, 1997] in addition to enabling comparisons of past climate with projected climate scenarios [e.g., Ault *et al.*, 2014; B. I. Cook *et al.*, 2015; Smerdon *et al.*, 2015].

Studies focused on the reconstruction of tree-ring-based paleohydrology (e.g., annual and season streamflow and floods) typically utilize proxies derived from tree-ring networks within or near the catchment region as predictors [e.g., Woodhouse *et al.*, 2006; St. George, 2010; Pederson *et al.*, 2012; Devineni *et al.*, 2013]. However, these networks are spatially irregular with record lengths varying across chronologies. An alternative to using spatially and temporally irregular tree-ring chronologies as model predictors is to use an existing derivative of these records, namely the Living Blended Drought Atlas (LBDA) [Cook *et al.*, 2010a]. The LBDA is a paleoclimate reconstruction of the summer (June–August) Palmer Drought Severity Index (PDSI) that is gridded across North America on a $0.5^\circ \times 0.5^\circ$ latitude/longitude grid with reconstructions dating back as far as 2000 years. These records are temporally complete over the Conterminous United States (CONUS) from 1473 onward. The LBDA, or its predecessor the North American Drought Atlas [Cook and Krusic, 2004], have been used to assess the frequency and spatial distribution of droughts over the past millennia [e.g., Herweijer *et al.*, 2007; B. I. Cook *et al.*, 2013].

2. A Proposal for Using PDSI to Reconstruct Streamflow

The intent of the modeling case study presented here is to develop a suitable framework with which streamflow within the CONUS may be reconstructed using a tree-ring-based reconstruction of the PDSI. In developing the modeling framework, we consider: (1) the constraints posed by the LBDA and implications for reconstructing streamflow; (2) possible temporal resolutions (monthly, seasonal, or annual) for direct streamflow reconstruction using the LBDA data; (3) how to best use local and far-field LBDA information for local streamflow reconstruction; and (4) provides insights from the 500 year reconstruction of the multisite Missouri River Basin flows as to the decadal and longer variability of streamflow in the region. Given the existence of the spatially and temporally complete LBDA record over the last 500 years covering the CONUS, we explore whether the LBDA, a reconstruction of PDSI using tree-ring chronologies, could be a reasonable predictor of streamflow variability. In this case, the variable to be reconstructed is annual streamflow with the aim of eventually reconstructing paleoclimate records of streamflow across the CONUS, an undertaking that has not previously been attempted using the LBDA or tree-rings.

The motivation for using the LBDA stems from our understanding that the growth of moisture-limited trees, from which the LBDA is derived, are in part governed by climatic forcings that drive soil moisture availability. That is, given a vector of unspecified climate variables, \mathbf{C}_t (where \mathbf{C} may be comprised of, but not limited to, climate variables such as temperature, rainfall, wind, soil moisture, and radiation) we can define PDSI as $PDSI_t = f_1(\mathbf{C}_t)$. Streamflow is also a derivative of a number of climate variables and can similarly be defined as $Q_t = f_2(\mathbf{C}_t)$. We seek to determine if it is possible to derive and fit a function f_3 that relates streamflow to PDSI where $Q_t = f_3(PDSI_t)$. Where suitable instrumental records of climate are available, we may derive f_1 and this has been approximated in part using methods such as the Thornthwaite potential evapotranspiration (PET) equation [Thornthwaite, 1948] and the Penman-Monteith PET equation [Monteith, 1965] to varying degrees of success [Lockwood, 1999; Sheffield *et al.*, 2012; Dai, 2013]. Consideration of the joint probability distributions $f(PDSI_t, \mathbf{C}_t)$ and $f(Q_t, PDSI_t)$ enables the vector of climate variables to be reconstructed by capitalizing on the climate-PDSI relationship and the tree-ring chronology-PDSI relationship given $f(\mathbf{C}_t|PDSI_t)f(PDSI_t|\text{tree-ring chronology}_t)$. Paleoclimate streamflow could similarly be derived by implementing f_2 , namely $f(Q_t|\mathbf{C}_t)f(\mathbf{C}_t|PDSI_t)f(PDSI_t|\text{tree-ring chronology}_t)$. However, the challenge in this approach is the selection of an appropriate vector of climate variables, many of which may be sparsely observed or unobserved in the instrumental record. Therefore, we consider modeling paleoclimate streamflow through $f(Q_t|PDSI_t)f(PDSI_t|\text{tree-ring chronology}_t)$. Since the reconstructed $PDSI_t$ in the LBDA is really $E[PDSI_t|\text{tree-ring chronology}_t]$, we start by considering $f(Q_t|PDSI_t)$, where Q_t is the streamflow at one or more locations in a river basin, and $PDSI_t$ represents a vector of LBDA values at the gridded locations of the LBDA that can be a potential predictor of the streamflows. The relationship can be developed using contemporaneous values of $PDSI_t$ and historical Q_t . Subsequently, we can apply this relationship to the paleo estimates of $PDSI_t$ recognizing that we could use the expected values of $PDSI_t$ reported in the LBDA, or simulations from the uncertainty distributions of $PDSI_t$ reported in the LBDA, as conditioning variables to derive sequences of Q_t .

A key motivation for using the LBDA is that it is spatially complete across CONUS over the past 500 years and a successful streamflow reconstruction would have significant value in assessing national water planning and use strategies and in investigating the different temporal and spatial structures in streamflow,

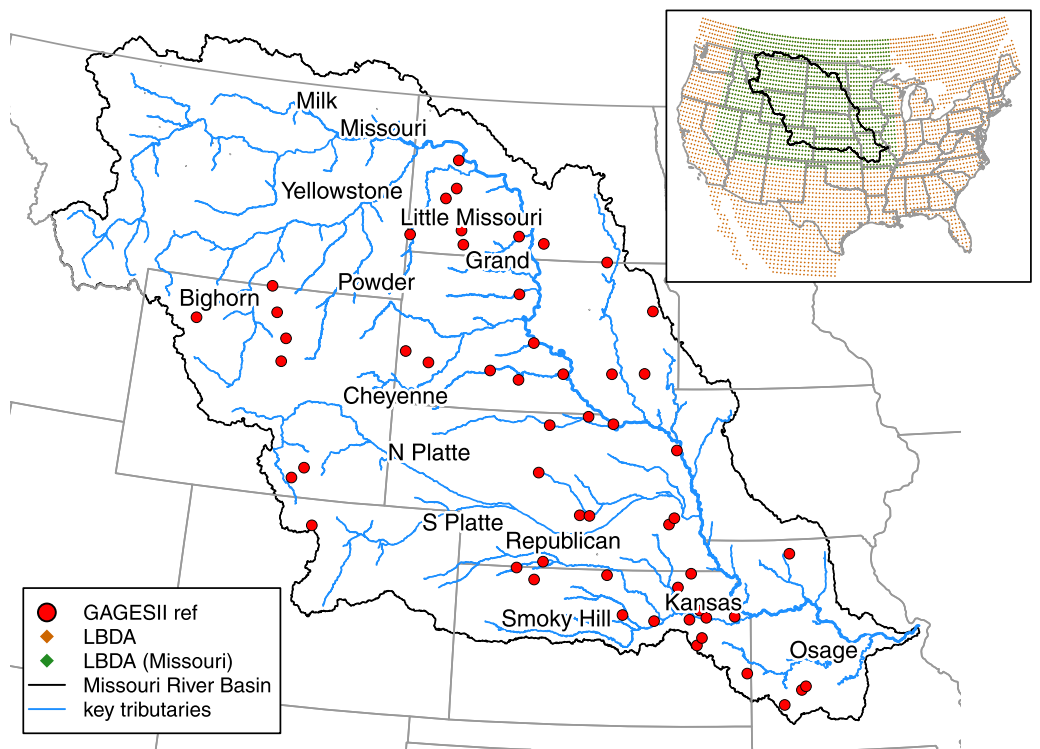


Figure 1. The Missouri River Basin, key tributaries, locations of gauged streamflow used in the analysis, and (inset) the LBDA grids used in the analysis. LBDA grids in the Missouri River Basin region shown in green.

which differ from the LBDA (see supporting information Figures S1 and S2). Relative to reconstructions that use tree rings within the river basin of interest, the use of a gridded proxy series to reconstruct watershed processes such as streamflow poses a novel challenge. The gridded LBDA series have high spatial correlation, since they rely on tree rings over a common radius of influence around each grid point, nominally 450 km in this case or roughly the correlation decay e-folding distance between grid points of the instrumental PDSI. A novel algorithm for reconstruction that uses local and global covariates for streamflow reconstruction using regularized canonical regression is developed and applied over the Missouri River Basin, as a test case. This provides a proof of concept at a subcontinental scale as to whether the approach is feasible. The Missouri River Basin was chosen as it contains the only major river headwaters in the western United States where extensive reconstructions of paleoclimate hydrology have not been undertaken [Driscoll, 2013] and also parallels current efforts to further develop tree-ring chronologies and streamflow reconstruction models using tree rings in the region [Pederson, 2013]. A description of the case study region and data are presented in the following section while section 4 presents initial diagnostics that inform the modeling approach developed in section 5. Section 5 details how the above proposal of using PDSI to reconstruct streamflow is implemented in the Missouri River Basin. Section 6 provides model verification results and summaries of the key modes of variability in the 500 year mean streamflow reconstructions of Missouri River Basin streamflow. The final section reviews outstanding questions as to modeling uncertainties, and the challenges for extending the model presented here to a national scale.

3. Case Study Region and Data

3.1. The Missouri River Basin

The Missouri River is the longest river and the second largest river basin in the United States, draining an area over 1.3 million km² that spans the southern portions of two Canadian provinces and 10 states in the United States (Missouri River basin boundary and key tributaries shown in Figure 1). The headwaters, which are largely snow-melt fed, are located in the Northern Rocky Mountains. These waters then flow through a largely semiarid region to its confluence with the Mississippi River near St. Louis, Missouri [Galat et al.,

2005]. Land use in the Missouri River Basin is dominated by agricultural activities including cropping and grazing which cover 95% of the region [U.S. Army Corps of Engineers, 2006], while the remaining land is used for recreation, transport, urban and industrial use including mining, and energy sector activities [Galat et al., 2005]. An improved perspective of streamflow variability would therefore be of benefit to the region in terms of managing and balancing the demands for water among the various sectors and users.

Precipitation and moisture availability in the Missouri River Basin are characterized by high precipitation in the western mountainous region, which averages over 1000 mm/yr to the drier region in the rain shadow east of the Rocky Mountains where average annual precipitation is less than 400 mm/yr. Precipitation increases toward the far eastern regions of the Missouri River Basin [Kunkel et al., 2013].

Winter precipitation in the northern Missouri River Basin and in the mountainous regions to the west is related to the El Niño Southern Oscillation (ENSO) signal from the preceding summer and autumn [Redmond and Koch, 1991]. El Niño teleconnections typically manifest as upper level anticyclonic high pressure cells over the northwestern U.S. and result in the northward displacement or splitting of the jet stream and anomalously dry conditions in the Missouri River Basin [Trenberth et al., 1988; Dettinger et al., 1998; Smith et al., 1998]. Conversely, La Niña events typically result in wetter conditions in this region. ENSO impacts are modulated by the decadal scale variability in the northern Pacific Ocean with warm decadal phases resulting in a deep Aleutian low and corresponding ridging over the western United States thereby enhancing El Niño conditions [Gershunov and Barnett, 1998; Brown and Comrie, 2004]. The enhancement of La Niña impacts by a cool phase in the northern Pacific decadal signature is particularly noticeable in the northern Missouri River Basin [Wise, 2010]. Both Pacific and Atlantic Ocean influences are seen in the Northern Great Plains with the Great Plains low level jet, originating from the Gulf of Mexico, enhancing summer precipitation in this region [Higgins et al., 1997].

3.2. Streamflow Data

Monthly streamflow data for the Missouri River Basin were obtained from the U. S. Geological Survey (USGS) Surface-Water Daily Data for the Nation (<http://nwis.waterdata.usgs.gov/nwis/sw>). The streamflow data are from stations included in the USGS's GAGES-II network [U.S. Geological Survey, 2011] within the Missouri River Basin boundary and are reference gauges identified by the USGS as the least-disturbed watersheds with minimal regulation. The selected gauges meet a criterion of data spanning 40 years with less than 5% missing data (Figure 1 and supporting information Table S1) and results in 55 streamflow gauges, 46 of which are also in the USGS Hydro Climatic Data Network.

Three of the selected stations had missing monthly values. These values were imputed using multiple imputation by chained equations (MICE) and a method of predictive mean matching [Buuren and Groothuis-Oudshoorn, 2011]. Monthly streamflow imputation was conducted using streamflow from the three closest stations and a cosine function to represent a seasonal signal. The number of repetitions in MICE was determined using a rule of thumb method proposed by White et al. [2011] and the multiple imputed monthly values were averaged across the repetitions.

Monthly data were aggregated into annual streamflow data using a calendar year instead of a water year because the average driest month of streamflow at most stations occurred in either December or January. Start and end years with incomplete data were excluded. The resulting annual data spans from 1929 to 2014 with annual record lengths varying between 39 and 85 years after aggregation. Streamflow was logarithmically transformed since that leads to a nearly Gaussian distribution for annual streamflow. Annual streamflow records of zero were replaced with half the minimum annual streamflow prior to the application of the log transform.

3.3. A Paleoclimate Record of North American Drought

The LBDA is an updated version of the seminal North American Drought Atlas (NADA) [Cook et al., 1999; Cook and Krusic, 2004; Cook et al., 2010a], which is a paleoclimate reconstruction of the summer (June–August—JJA) PDSI based on a network of tree-ring chronologies. The LBDA has a spatial resolution of $0.5^\circ \times 0.5^\circ$ latitude/longitude and incorporates information from 1845 tree-ring chronologies, an improvement over previous NADA versions that were informed by fewer tree-ring chronologies and were calculated over coarser grids [Cook et al., 1999; Cook et al., 2004]. The LBDA is spatially complete over the CONUS region from 1473 to 2005 and includes instrumental data from 1979 onward. A region of the LBDA ranging from

23°N to 52°N and 125°W to 66°W (see green dots in Figure 1) was extracted for the analysis. This broad region extending beyond the CONUS region was selected to capture patterns of LBDA variability relevant to the CONUS. A comparative analysis between an instrumental-based gridded PDSI data set and the LBDA showed that they are highly correlated, with correlation values significant at the 99% level and similar variance (results not shown here). The instrumental LBDA data post-1978 were therefore also included in the modeling analysis performed here.

4. Initial Diagnostic Analyses

Initial diagnostic analyses were performed using both parametric and nonparametric correlations (Pearson and Kendall correlations, respectively) between the LBDA and the log-normal streamflow series. The two correlations measures yielded similar results suggesting a near-Gaussian linear dependency [Pizarro and Lall, 2002]. Different levels of temporal aggregation were tested including monthly, rolling seasonal, biseasonal, and annual streamflow. Different representations of the LBDA were also tested including using the LBDA grid located nearest to each streamflow gauge, using LBDA grids surrounding each streamflow gauge within a given diameter, and principal components (PCs) [Jolliffe, 2002] and archetype analysis [Cutler and Breiman, 1994] of U.S.-wide and Missouri River Basin region LBDA (see orange and green diamonds, respectively, in Figure 1). An annual temporal aggregation of streamflow was found to produce the strongest signal (Figure 2 showing correlation results between streamflow gauges in the Missouri River Basin and the nearest LBDA grid and PCs of U.S.-wide LBDA). Diagnostic tests using the nearest LBDA grid were superior and reflects the ability of the point-by-point regression method used for the LBDA to preserve local climate details in the PDSI reconstructions that are also related to streamflow.

High correlations were also noted for some streamflow stations with LBDA in the surrounding region (see supporting information) particularly for streamflow records with weaker correlations with the nearest grid (e.g., gauges in south-central North Dakota and on the border of Nebraska and Kansas). We therefore considered information from LBDA grids within a 450 km radius consistent with the tree chronology search radius used to form the LBDA. Furthermore, given that large-scale climate and weather patterns influence local hydroclimatic conditions [Woodhouse et al., 2002], one needs to also consider the relationships with these larger modes of variability.

Correlations between streamflow and the first eight PCs of LBDA grids across the United States (LBDA locations shown in Figure 1, correlations in Figure 2, and PC loading patterns shown in Figure 3) show that the Missouri River Basin streamflow is correlated with PC1, a PC representing overall U.S. LBDA variability. However, these correlations are weak in comparison with correlations with the nearest LBDA grid. The north/south loading pattern of PC 2 is reflected in the change in correlation sign for stations north and south of the Nebraska and Kansas border. Similarly, the east-west difference in the loadings of PC3 leads to strong positive correlations in the downstream reaches of the Basin in Kansas and Missouri and negative correlations in Nebraska and Wyoming. The correlation results between streamflow and PCs of CONUS LBDA suggest that the large-scale modes of variability could provide additional information for modeling streamflow. Further details of the eight PCs of the CONUS LBDA and selection methods are provided in supporting information.

5. Modeling Approach and Performance Metrics

Here, we present a suite of plausible methods that could be implemented to model streamflow using the LBDA as the covariate(s) (section 5.1). We justify the selection of a model that incorporates the use of regularized canonical correlation (rCCA), which is further described in section 5.2. A description of the model performance metrics is provided in section 5.3.

5.1. Model Design and Preliminary Model Assessment

We seek to use log-linear models to quantify the relationship between streamflow at individual gauges and a suite of site-specific LBDA records to facilitate a paleoclimate reconstruction of streamflow in the Missouri River Basin. Keeping in mind the application to streamflow record extension using the reconstructed PDSI values available in the LBDA, we consider the following steps:

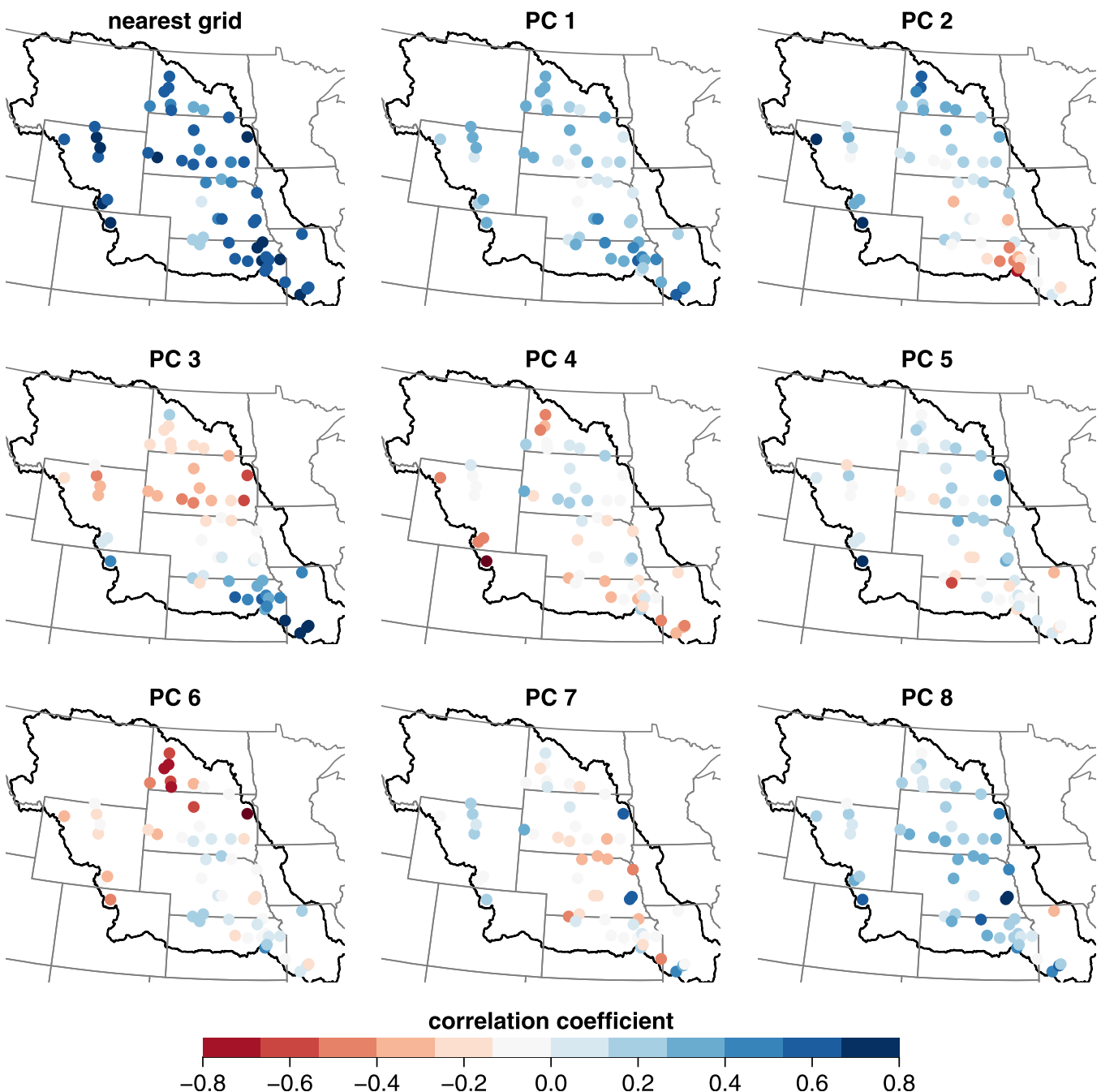


Figure 2. Pearson correlation between annual streamflow and (a) closest LBDA grid (b)-(i) PC1-PC8 of U.S.-wide LBDA.

1. Instrumental Period (32–77 years at 55 locations): Use LBDA reconstructed PDSI to estimate the relationship between log transformed annual streamflow and a selection of LBDA records specific to the target streamflow site, namely $f(\ln(Q_t)|PDSI_t)$, where $PDSI_t$ is really the expected value of PDSI informed by the tree-ring chronologies, $E[PDSI_t|tree-ring\ chronology_t]$, from 1929 to 2005 to maximize the overlap between the two sets of variables.
2. Paleo Period (1473–1929): Use $f(\ln(Q_t)|PDSI_t)$ estimated in the previous step with the LBDA reconstructed PDSI, $E[PDSI_t|tree-ring\ chronology_t]$, to estimate $\ln(Q_t)$ prior to 1929 (estimates of $\ln(Q_t)$ post 1929 will also be shown for comparison).

Several reconstruction model designs were considered given the initial diagnostic results. These included:

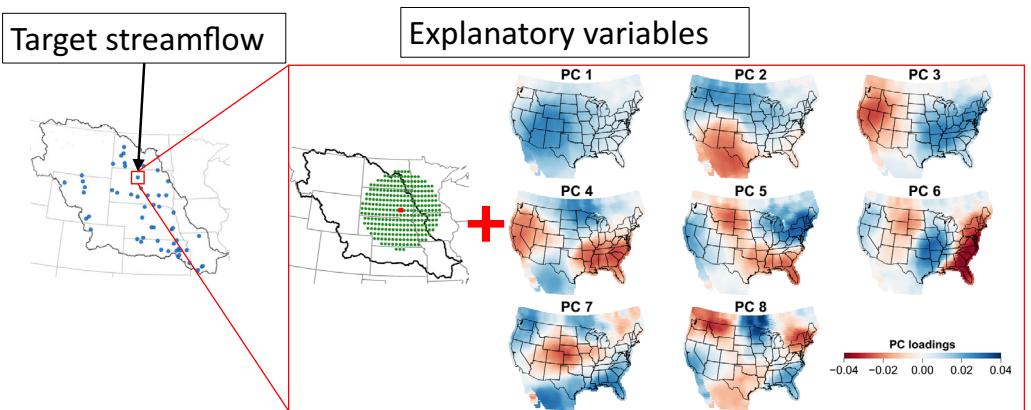


Figure 3. Schematic of LBDA information to be included in the reconstruction model of one streamflow station in the Missouri River Basin. The model inputs are the LBDA within a 450 km radius and the first 8 PCs of U.S.-wide LBDA.

1. Developing one model for each streamflow station with predictors comprised of either:
 - 1a. the LBDA grid located closest to the streamflow gauge;
 - 1b. PCs of the LBDA from a region around the Missouri River Basin (Figure 1, green diamonds) within a multilinear model framework;
 - 1c. canonical correlation analysis with regularization(rCCA described in section 5.2) using LBDA grids within a 450 km radius; or
 - 1d. rCCA using LBDA grids within a 450 km radius in addition to the retained PCs of CONUS-wide LBDA.
2. Developing one model for all streamflow stations with predictors comprised of either:
 - 2a. PCs of both streamflow and CONUS-wide LBDA; or
 - 2b. rCCA using streamflow and LBDA information from either the Missouri River Basin region or the CONUS region.

The fine resolution, gridded LBDA data result in a large number of highly correlated, potential predictors in all of the model designs considered with the exception of 1a. Given the $0.5^\circ \times 0.5^\circ$ resolution of the LBDA data, if a reconstruction of streamflow at a single gauge is considered using only a 450 km radius of surrounding LBDA data, one has around 300 potential predictors including the leading eight CONUS LBDA PCs. The length of annual streamflow records in the Missouri River Basin ranges from 39 to 85 years, and thus it is clear that the number of potential predictors is significantly greater than the number of observations available to fit the model. Of course, if one were to consider a model with a simultaneous reconstruction of all the streamflow records, the dimension of the estimation problem becomes even more challenging. Consequently, this is the first issue considered in model development.

A single reconstruction model would be advantageous in its ability to consider all streamflow stations at once rather than fitting 55 individual models. However, the varying streamflow record lengths and differences in record periods would have resulted in large uncertainties as a large degree of annual streamflow imputation would have been required. As a result, model designs under option 2 were not further examined.

A cursory comparison of the viable models was conducted by comparing the coefficient of determination for each fitted model. The development of individual models for each streamflow gauge using either model 1a (the closest LBDA grid) or 1b (PCs of the LBDA in a region around the Missouri River Basin) resulted in acceptable models of streamflow (mean adjusted R^2 across the two models were 0.37 and 0.33, respectively). However, the spatially complete LBDA presents the opportunity to include a wider variety of local and large-scale information and these models (model designs 1c and 1d) were superior to the simpler models (model designs 1a and 1b). In addition, rCCA using both local and CONUS-wide information (model 1d) resulted in slightly improved model results (mean adjusted R^2 of 0.74 across all individual station models) over using only local information (model 1c, mean adjusted R^2 of 0.71). We therefore selected model 1d (rCCA using LBDA grids within a 450 km radius in addition to the retained PCs of CONUS-wide LBDA) for further analysis. A schematic of the data used to fit this model is shown in Figure 3, while a more detailed description of rCCA is provided in section 5.2.

5.2. Regularized Canonical Correlation Analysis

Methods such as principal component analysis (PCA) [Jolliffe, 2002], archetype analysis (AA, Cutler and Breiman, 1994; Stone and Cutler, 1996; Steinschneider and Lall, 2015], and canonical correlation analysis (CCA) [Hotelling, 1936] are typically used for dimension reduction in this setting. Given that the number of potential predictors exceeds the number of observations, their high mutual correlation (>0.95 for many of the adjacent grids), and an interest in exploring a multivariate streamflow response, we explore the use of regularized canonical correlation where the regularization procedure is akin to ridge regression [De Bie and De Moor, 2003]. Regularized canonical correlation was selected for use here to capitalize on its ability to tailor the dimension reduction process to maximize the correlation between the explanatory and target variables (in contrast to PCA where the explanatory and target variable relationship is not considered).

Canonical correlation was introduced by Hotelling [1936] as a method of linearly transforming two vector variables to canonical form to maximize the correlation between them. Consider two sets of random variables represented by two matrices \mathbf{X} and \mathbf{Y} . \mathbf{X} is a $n \times p$ matrix where $\mathbf{X} = [\mathbf{x}_1, \dots, \mathbf{x}_p]$ containing n observations at p different locations, while \mathbf{Y} is a $n \times q$ matrix where $\mathbf{Y} = [\mathbf{y}_1, \dots, \mathbf{y}_q]$ containing n observations at q different locations. Both \mathbf{X} and \mathbf{Y} have finite variance matrices represented by Σ_{XX} and Σ_{YY} , respectively. The covariance matrix between \mathbf{X} and \mathbf{Y} is Σ_{XY} while the covariance matrix between \mathbf{Y} and \mathbf{X} is Σ_{YX} . In this application, \mathbf{X} consists of the LBDA inputs specific to each streamflow gauge and \mathbf{Y} is the streamflow at one station (i.e., p is large and $q = 1$). Canonical correlation analysis involves rotating the coordinate axes of both \mathbf{X} and \mathbf{Y} to new coordinate systems in order to clearly exhibit correlation between \mathbf{X} and \mathbf{Y} . An arbitrary linear combination could be $\mathbf{U} = \mathbf{X} \times \boldsymbol{\alpha}$ and $\mathbf{V} = \mathbf{Y} \times \boldsymbol{\gamma}$ such that the correlation between \mathbf{U} and \mathbf{V} is maximized. \mathbf{U} and \mathbf{V} yield the first pair of canonical variates, while $\boldsymbol{\alpha}$ and $\boldsymbol{\gamma}$ are the vectors of canonical weights of length p and q , respectively. This process may be repeated subject to the constraint that following pairs of canonical variates are orthogonal to previous pairs with a maximum of $\min(p, q)$ pairs obtained. In this application, the model of streamflow is applied station by station and therefore only one pair of canonical variates are calculated and the first canonical variate of the LBDA is used to fit the model of streamflow.

The correlation of successive pairs of canonical variates can be found using an eigen decomposition of $\Sigma_{XX}^{-1} \Sigma_{XY} \Sigma_{YY}^{-1} \Sigma_{YX}$ and $\Sigma_{YY}^{-1} \Sigma_{YX} \Sigma_{XX}^{-1} \Sigma_{XY}$. The resulting $\min(p, q)$ eigenvalues are common to both and the square root of the eigenvalues yield the canonical correlation. The eigenvectors of $\Sigma_{XX}^{-1} \Sigma_{XY} \Sigma_{YY}^{-1} \Sigma_{YX}$ and $\Sigma_{YY}^{-1} \Sigma_{YX} \Sigma_{XX}^{-1} \Sigma_{XY}$, respectively, yield the canonical weights $\boldsymbol{\alpha}$ and $\boldsymbol{\gamma}$ that are used to transform \mathbf{X} and \mathbf{Y} . These weights are akin to the beta values in a multiple linear regression. Transforms using the i th eigenvector result in correlations corresponding to the square root of the i th eigenvalue. Here, the weight for \mathbf{Y} (streamflow) is 1 and the weights for \mathbf{X} (LBDA) are given by the first eigenvector of $\Sigma_{YY}^{-1} \Sigma_{YX} \Sigma_{XX}^{-1} \Sigma_{XY}$.

We employ regularization of the CCA process to address the issue of a large number of predictors relative to the number of observations [Vinod, 1976]. Regularization is a smoothing process where a "roughness penalty," also known as the regularization parameter (λ), is introduced by converting Σ_{YY} and Σ_{XX} to $\Sigma_{YY} + \lambda_y \mathbf{I}$ and $\Sigma_{XX} + \lambda_x \mathbf{I}$, respectively [Leurgans et al., 1993] and is similar to the technique of ridge regression [De Bie and De Moor, 2003]. Values of λ range between 0 and 1 with larger λ values indicating a higher degree of smoothing. Regularization also enables the process of matrix inversion to be stabilized. A suitable value of λ is determined using a leave one out cross validation score, where λ_x and λ_y are selected such that the correlation between the transformed data sets are maximized while the degrees of freedom used (as defined by Dijkstra [2014]) are limited to a maximum of $n - 10$. If the criteria for the maximum degrees of freedom could not be achieved λ was set to one, otherwise λ was evaluated to two significant figures. No regularization was required for the single variable streamflow, while the LBDA was heavily regularized in almost all cases (Figure 4). rCCA was executed in R using the R package "CCA" by González et al. [2008] and is freely available from the Comprehensive R Archive Network (CRAN <https://cran.r-project.org/>).

5.3. Model Performance Metrics

The performance of the model selected for further analysis includes verification using a leave-k-out cross-validation procedure. Ten percent of the data (between 3 and 8 years out of a total of 32 and 77 years of streamflow data overlapping the LBDA record) are randomly selected and withheld from model fitting. These values are then predicted from the model fit to the balance of the data. The entire process is

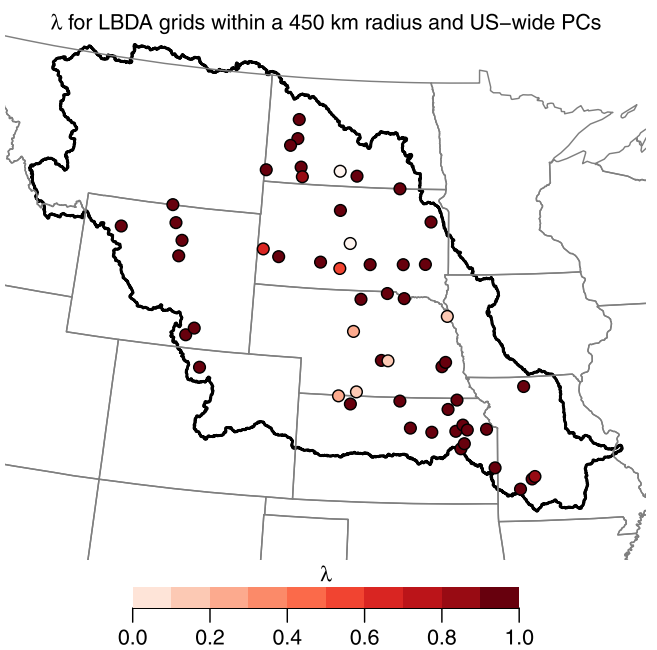


Figure 4. CCA regularization parameter values for the explanatory variables (LBDA grids within a 450 km radius and CONUS-wide PCs) for each model of LBDA and streamflow.

while x and \hat{x} are the means of the observed streamflow in the validation and calibration periods, respectively.

6. Results

A log-linear model was individually fitted to each streamflow gauge using logarithmically transformed streamflow and the first canonical variate of the LBDA inputs (schematic of inputs shown in Figure 3) using rCCA. The models were tested using a cross-validation procedure and calibration and verification metrics, as described in section 5.3 were calculated. Finally, an overall assessment of the dominant modes of temporal variability in reconstructed streamflow variability in the Missouri River Basin was made using a frequency wavelet analysis on the leading PCs of reconstructed streamflow.

6.1. Model Results

Streamflow at each of the 55 stations in the Missouri River Basin was constructed using a least squares regression model of natural-log streamflow and the first regularized canonical variate of the combined LBDA grids within a 450 km radius and first eight PCs of U.S.-wide LBDA as the predictor variable. All results for modeled and reconstructed streamflow are shown in log space, while verification statistics are also calculated for logarithmic streamflow. An example of the input and modeled streamflow is shown for one streamflow station calibrated using data from Turkey Creek near Seneca (Figure 5). A summary of modeled streamflow results and summary statistics of the residuals for both calibrated and verified streamflow across all 100 calibration and verification sets are provided in supporting information.

The rCCA linear model resulted in 55 models with adjusted R^2 values ranging between 0.56 and 0.90. The model residuals were near normal at almost all stations with the exception of some stations with small catchment regions showing near-uniform residuals. In each streamflow model, the magnitude of rCCA loadings for the eight PCs of CONUS LBDA were similar to those of the ~300 local LBDA grids indicating that information from the eight PCs of CONUS LBDA did not dominate the reconstruction.

repeated 100 times, thus providing a set of 100 k-fold cross-validation samples. A comparison of the model residuals resulting from both calibrated and verified model inputs is made for the 100 cross-validation samples. The coefficient of efficiency (CE) and the reduction of error (RE) [Cook *et al.*, 1994; Wilson *et al.*, 2010] are additional metrics calculated to verify the model. Both CE and RE are similar to the Nash-Sutcliffe efficiency test; however, the metrics are normalized using the mean of the verification and calibration data, respectively. Namely, CE is defined as

$$CE = 1 - \frac{\sum_{i=1}^n (x_i - \hat{x}_i)^2}{\sum_{i=1}^n (x_i - \bar{x}_v)^2}$$

while RE is defined as

$$RE = 1 - \frac{\sum_{i=1}^n (x_i - \hat{x}_i)^2}{\sum_{i=1}^n (x_i - \bar{x}_c)^2}$$

where x_i and x are the observed and modeled streamflows, respectively,

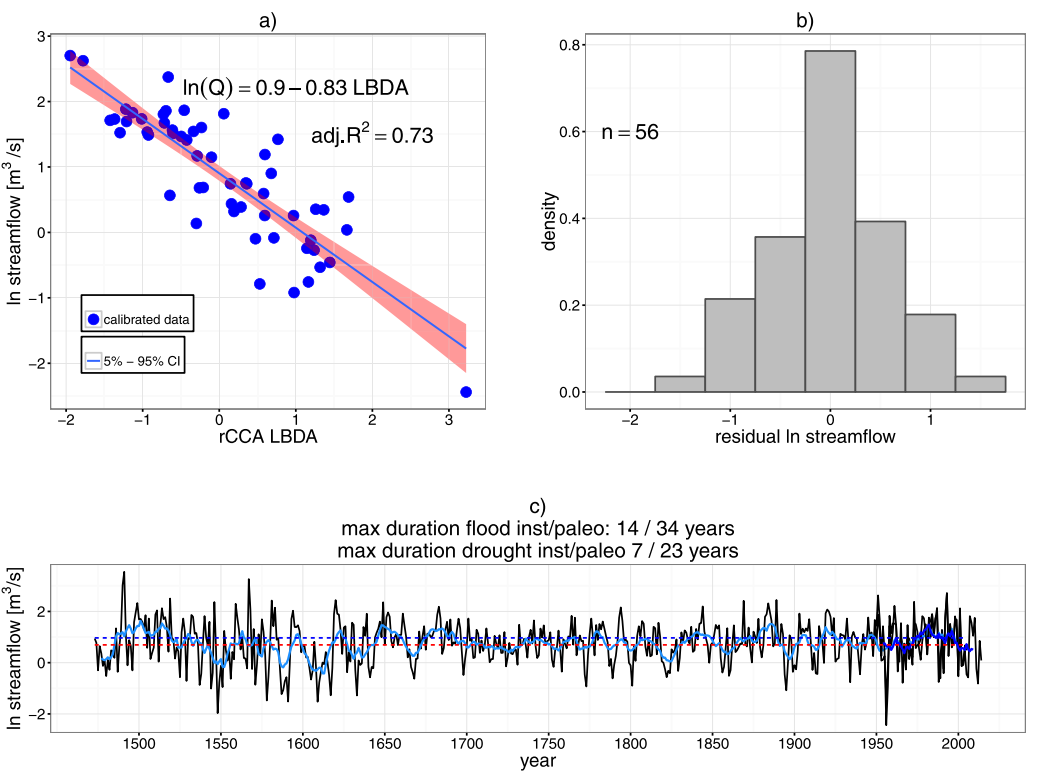


Figure 5. Model results for Turkey Creek near Seneca (USGS gauge number 06814000) calibrated using all available data and the first canonical variate of the LBDA inputs (a) input (dots) and modeled (line) natural log streamflow showing 5th–95th prediction interval, (b) histogram of model residuals, and (c) flood and drought persistence gauged by a threshold of mean $\pm 0.5SD$ of 10 year running average (blue lines—light blue line is the reconstructed ten year moving average).

6.2. Model Validation

The predictive power of the model was assessed by calculating the coefficient of efficiency (CE) and reduction of error (RE) for all cross validations. The median CE and RE values are shown in Figures 6a and 6b, respectively, while distributions of the values are shown in box plots in supporting information. CE and RE values range from $-\infty$ to 1, with values over 0 indicating that the model predictions are more accurate than the respective climatology used for each statistic.

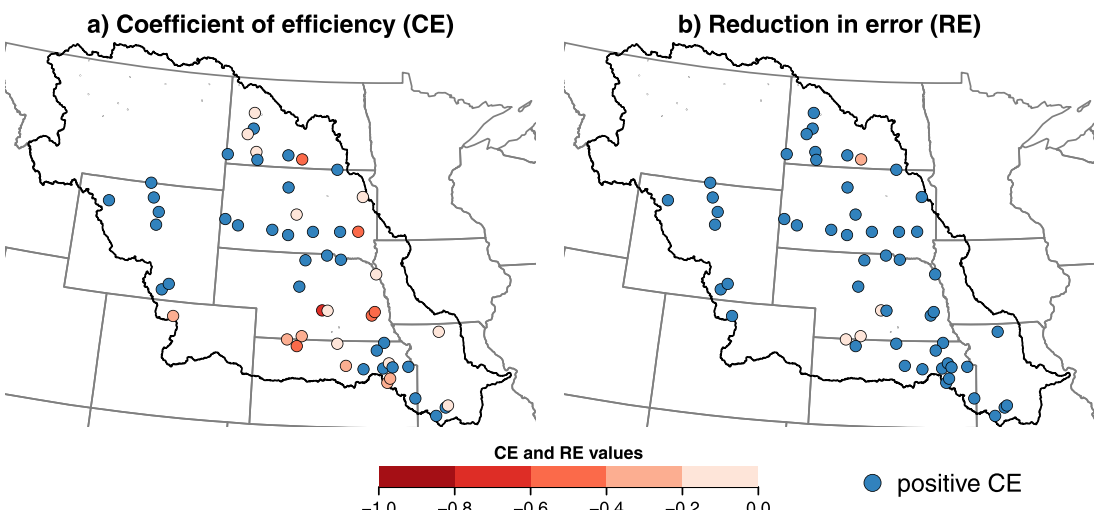


Figure 6. Median values of (a) CE and (b) RE values for cross-validated models of the 55 Missouri River Basin streamflow stations.

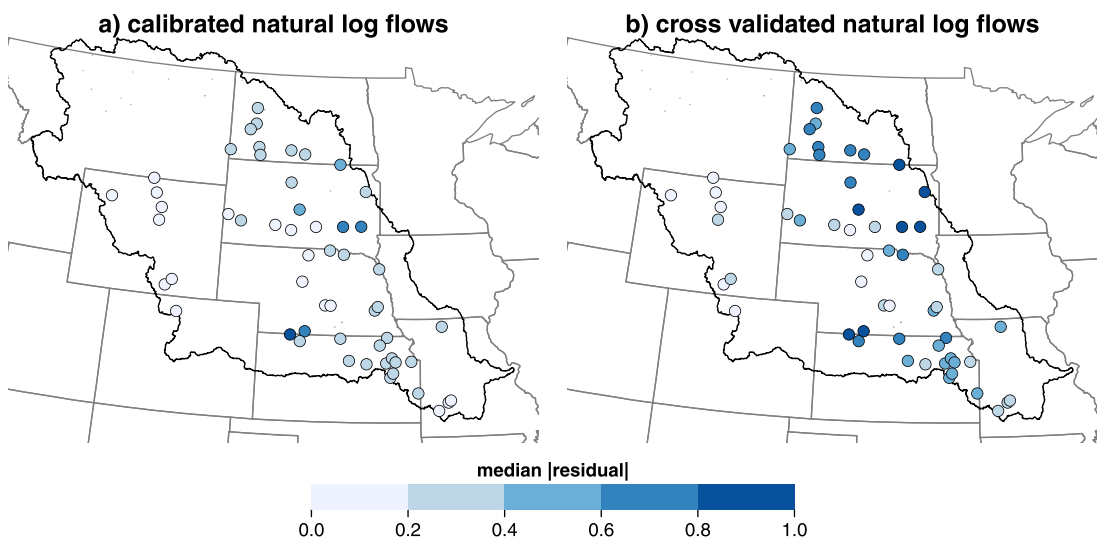


Figure 7. Median cross validated model residuals (absolute value) for (a) calibrated and (b) verified natural log streamflow inputs at the 55 Missouri River Basin streamflow stations. Cross validations were repeated 100 times.

The CE values in Figure 6 indicate that many of the streamflow models are able to provide median streamflow predictions with greater accuracy than the climatology of the withheld data. The RE values likewise suggest that the models are able to predict the withheld values with greater accuracy than the climatology of the calibrated values at most stations. The combined CE and RE results suggest there is some skill in reconstructing paleoclimate streamflow using the LBDA.

A comparison of the distribution of residuals resulting from calibrated values versus validated values was also made using the 100 repetitions of the k-fold cross validation test. The median and the range of the cross-validated absolute residuals are modestly larger than that of the absolute residuals during the fitting process. The differences, accounting for the sample sizes, are not statistically significant in over 90% of 100 cross validated results (using a two-sided t-test and a null hypothesis that the true difference between the means is zero and alpha = 0.05). The median values of the cross validated residuals are shown in Figure 7, while box plots showing the distribution of the cross validated residuals are shown in supporting information. A summary of the reconstruction is presented in section 6.3 using PCs of the streamflow reconstructed at the 55 stations.

6.3. Reconstructed Streamflow Analysis

Mean annual streamflow was reconstructed for all 55 stations in the Missouri River Basin (data available in Ho *et al.* [2016]). PCA was used to extract the leading modes of variability from the reconstructed Missouri River Basin natural log streamflow at all 55 stations. A combined assessment of the PCs using North's Rule of Thumb and a scree plot showed adjacent degenerate eigenvalues pairs for PCs of order 4 and higher and discontinuities at PC4, respectively (shown in supporting information). Furthermore, the spatial pattern of PC4 was difficult to interpret and therefore only the first three PCs are shown in Figure 8.

Negative streamflow anomalies coinciding with the 1930s dust bowl drought and 1950s drought are evident in PC1, which has a positive loading pattern across all stations in the Missouri River Basin (Figure 8). The 1950s drought had more severe impacts in the southern half of the Missouri River Basin [Piechota and Dracup, 1996; Cole *et al.*, 2002; Andreadis *et al.*, 2005; Cook *et al.*, 2009] and this is detected in PC2 that is comprised of positive loadings in the southern half of the Basin. The Civil War drought, which largely impacted the Central Plains region from the mid-1850s to mid-1860s [Herweijer *et al.*, 2006], is also evident in PC2.

The severity of these droughts had wide ranging impacts on ecological states, agricultural produce, and social activities and are often used as benchmark droughts to which contemporary droughts are compared [Breshears *et al.*, 2005; Hornbeck, 2009]. However, the streamflow reconstructions suggest periods where

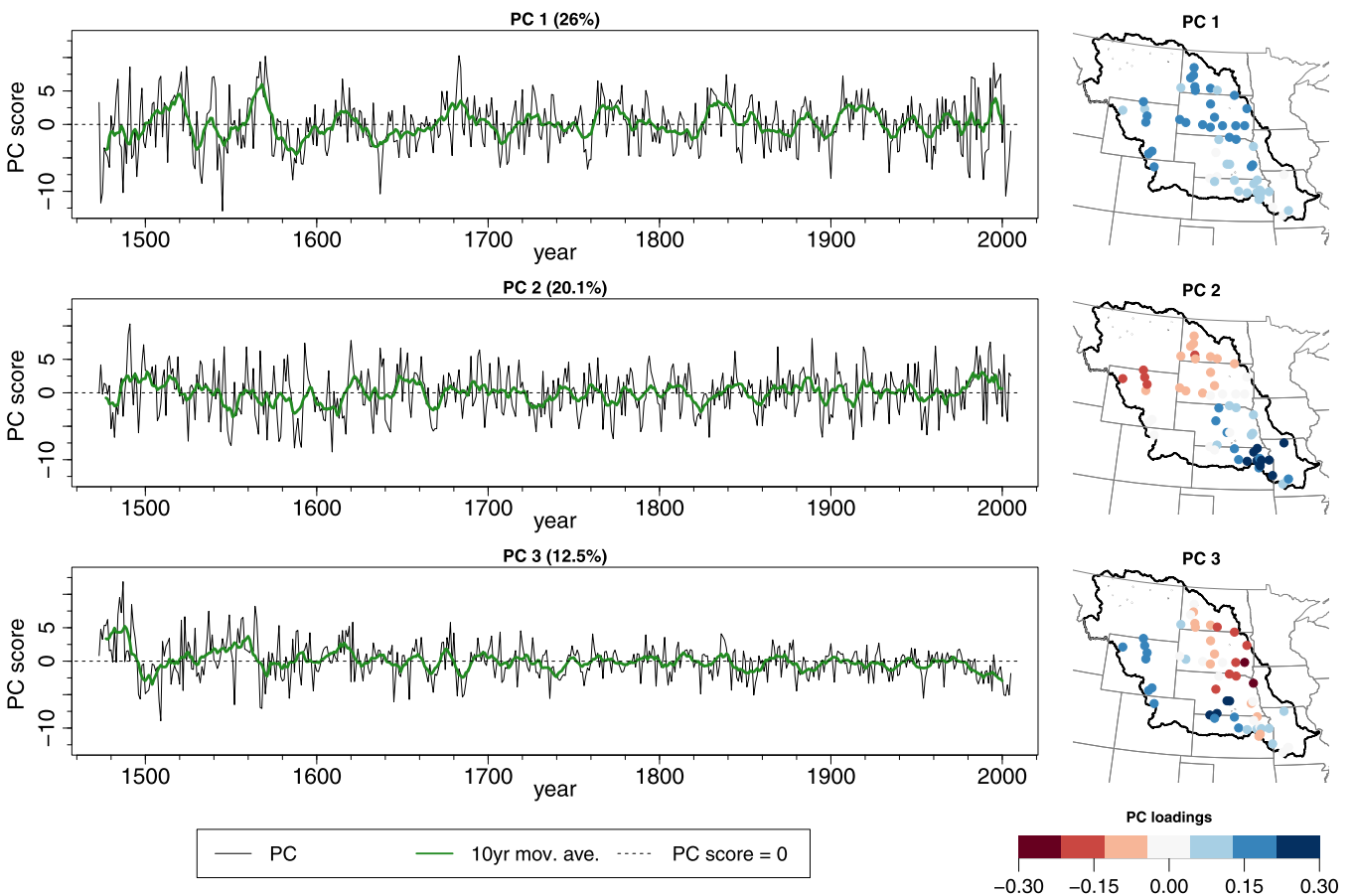


Figure 8. Annual (black) and 10 year moving average (green line) of the first four PCs of reconstructed mean natural log streamflow in the Missouri River Basin (left) with percentage variance explained shown in parenthesis and the corresponding loading patterns (right).

streamflow deficits may have been more severe than any of these historical droughts. For example, the late 1540s, 1590s, and late 1750s all show negative streamflow anomalies in both PC1 and PC2 (26% and 20.1% variability explained, respectively) that are of similar or greater magnitude than the streamflow deficits associated with the Civil War, Dust Bowl, or 1950s droughts. Drought durations were also longer when assessed in the context of streamflow variability over the past 500 years. A threshold of above or below 0.5 standard deviation in decadal streamflow at each station was used as an approximation of flood and drought regimes, respectively. The maximum duration of continuous periods of either flood or drought regimes were found to be longer in the majority of stations investigated as demonstrated in Figure 5c that shows the reconstructed annual and decadal streamflow at Turkey Creek and the longest duration drought and flood regime for the station.

PC3 (12.5% variability explained) is a mode of variability largely influenced by differences in streamflow variability between the Rocky Mountains regions and the remainder of the Missouri River Basin. The apparent increase in variability in the 1500s and 1600s in PC3 suggests that differences in streamflow variability between the Rocky Mountains regions and the plains region may have been more pronounced during these two centuries.

PC2 of the reconstructed streamflow has positive loadings in the southern Missouri River Basin. This PC shows an extended period of below average flows, with the exception of a couple of years, in the first two decades of the 1600s and is evident in individual streamflow reconstructions around the border of Nebraska and South Dakota and in Kansas. A similar persistence of decadal-scale low flows are not featured in the instrumental record, suggesting that successive years of low streamflow have persisted for longer periods than what has been observed in historical records.

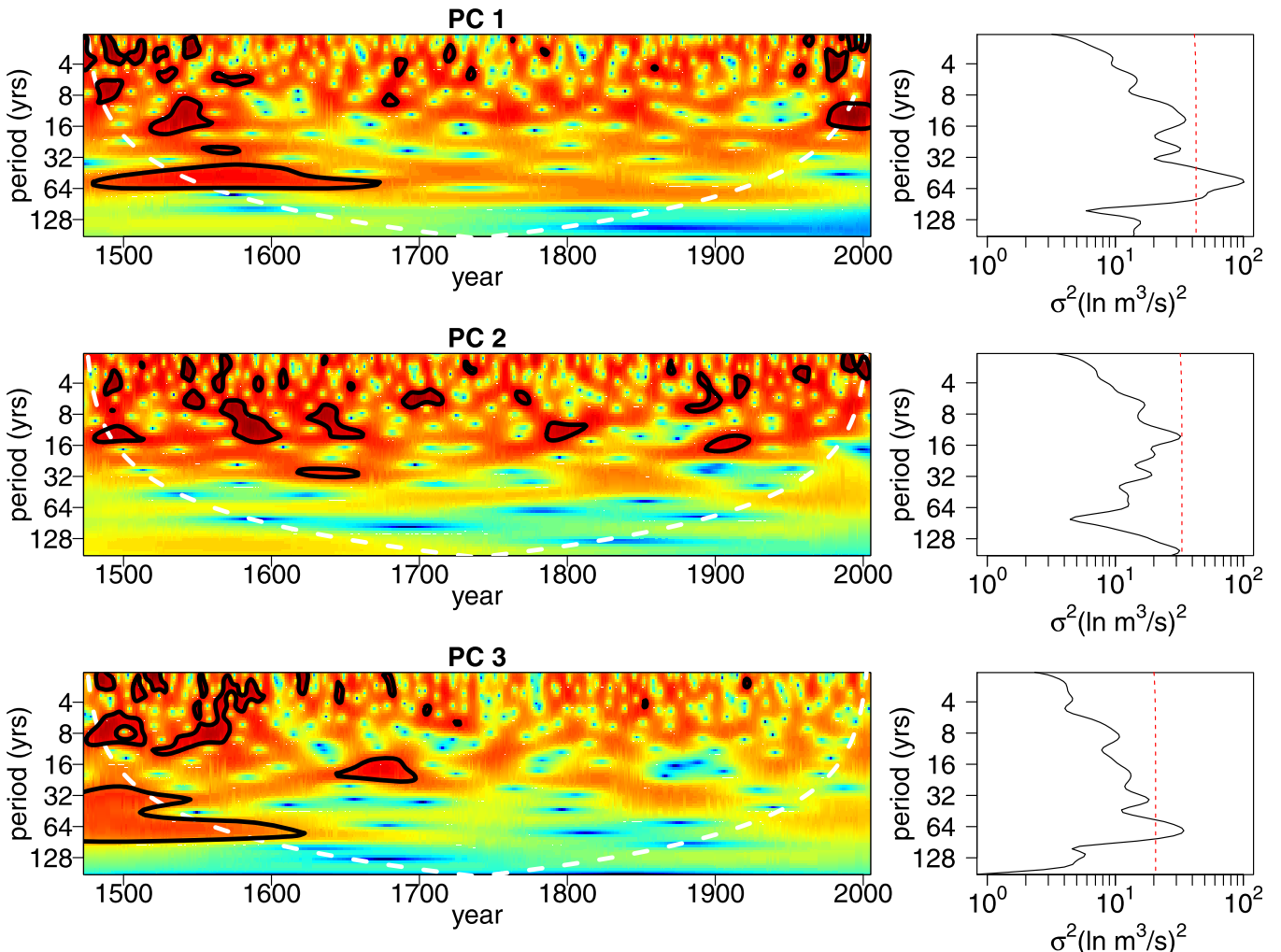


Figure 9. Wavelet transforms of PC 1–3 of reconstructed log streamflow in the Missouri River Basin from 1473 to 2005 (left), black lines show 95% significance level, dashed white line shows cone of influence under which edge effects may influence the results, and the time-averaged global wavelet spectra (right) with red dashed line showing 95% confidence level for the wavelet transform using a white noise background spectrum.

The PCs of the reconstructed streamflow also show several periods where annual flows are larger than the maximum instrumental streamflow. Periods of anomalously high streamflow include the 1560s for PC 1 and the early 1490s for PC 2 and 3. These periods coincide with high positive reconstructed PDSI values particularly in the lower Missouri Basin region and along the middle and southern Rocky Mountains in the early 1490s and positive PDSI values across most of the interior plains. Anomalously large streamflow during the 1560s were reconstructed at stream gauges around the interior plains regions from tributaries that join the Missouri River in North and South Dakota (e.g., Cannonball, Grand, and White Rivers). However, anomalously high streamflow around the 1560s was not reconstructed for either the Platte or Yellowstone rivers suggesting that the increase in streamflow may have resulted from weather systems delivering moisture in the upper Interior Plains (North and South Dakota), but not in the Rocky Mountains region.

In order to quantitatively assess the temporal modes of variability implied by the PCs, a continuous wavelet transform was applied to identify key periodicities in the main modes of reconstructed streamflow variability. Wavelet transforms for PCs 1–3 along with their global wavelet spectra are shown in Figure 9. The wavelet transforms were implemented using the Morlet wavelet function as the mother wavelet and padded with zeros to limit the edge effects of the wavelet analysis [Torrence and Compo, 1998].

All PCs show decadal-scale variability in the 1500s and 1600s, which is significant at the 95% level against white noise for PC 1 and 3. Interestingly, none of the wavelet spectra show a consistent mode of variability

that coincides with an El Niño Southern Oscillation frequency (2–7 years) [Allan, 2000]. In addition, previously identified periods of decadal-scale variability in paleoclimate reconstructions of the Pacific Decadal Oscillation [Gedalof and Smith, 2001; MacDonald and Case, 2005] are not reproduced in the streamflow reconstruction. The multidecadal-scale variability seen in PC1 and PC3 around the 16th century suggest that the persistence of drought and pluvial events was longer around this period compared with historic records and is reflected in previous reconstructions of persistent drought during this period [Woodhouse and Overpeck, 1998] and in nearby regions [Meko *et al.*, 1995]. A similar pattern of multidecadal-scale variability is also seen in the PCs of LBDA grids within the Missouri River Basin around the 16th century (results not shown here).

7. Discussion and Conclusions

Human activities and social processes are irrefutably intertwined with the hydrological cycle with each influencing and affecting the behavior of the other [Matalas *et al.*, 1982]. Consequently, hydrologic investigations need to occur at spatial scales that encompass the social and political regions influencing how water is stored, used, and transported. This requirement necessitates a broader spatial scale to be considered beyond the watershed scale typically addressed in hydrologic assessments [Vogel *et al.*, 2015]. Spatially and temporally broad measures of hydroclimatic variability such as the LBDA provide opportunities to conduct such assessments.

We used the LBDA to demonstrate a method of reconstructing mean annual streamflow in the Missouri River Basin from 1473 to 2005 in order to facilitate a future reconstruction of streamflow across the CONUS. The rCCA approach enabled a large degree of spatially coherent information in the LBDA to be condensed via linear transforms into a canonical variate that explained the majority of information in the target streamflow. The additional regularization step addressed the issue of an ill-posed problem where the number of variables far exceeded the number of observations. Regularization addressed potential issues with overfitting of the model and subsequent poor predictability of uncalibrated values. This site-by-site approach, opposed to a multisite model, avoided data issues where streamflow records were not concurrently available at all sites. The method also tailored the LBDA information included in the model to each unique site and therefore has the potential to be applied to any individual streamflow site in the United States and, potentially, any streamflow site in North America where there are useful reconstructions in the LBDA.

The analysis of streamflow variability in the Missouri River Basin over the past 500 years was, however, limited by the absence of streamflow gauges in the headwaters of the Missouri River. Based on the selection criteria used here, there are no gauges located upstream of Fort Peck Lake and only one gauge in Montana was included in the analysis. The dearth of gauges in this region therefore omits potentially critical information when drawing conclusions regarding regional streamflow variability as presented in section 6.3. Future analyses could seek to include additional streamflow gauges, potentially drawing on nonreference gauges from the GAGESII database and other sources. While nonreference GAGESII gauges are located within disturbed catchments with potentially regulated streams, it may be plausible that these measurements would still preserve the signatures of interannual streamflow variability which we seek to recover. Encouragingly, the headwater regions of the Missouri River Basin contain a relatively dense network of tree-ring chronologies that would improve the fidelity of both PDSI and subsequent streamflow reconstructions. Furthermore, efforts towards expanding this tree-ring network are currently been made with a view to target and improve Missouri River Basin streamflow reconstructions [Pederson, 2013].

Dendrochronological studies for the purposes of climate reconstruction typically use a targeted sampling method whereby old living trees are selected for sampling to maximize the length of reconstruction and the location of sampling is chosen to ensure that tree growth is largely limited by the climatic factors of interest for reconstruction [Speer, 2010]. Over 50 different tree species were used in the formulation of the LBDA, however, species was not a determinant for inclusion in the LBDA. Rather, the tree-ring chronologies specifically selected for use in reconstruction were those that were best correlated with available soil moisture as modeled a priori by PDSI and this was done using a method of point-by-point regression that ensures that the selected chronologies were likely to have a causal association with the gridded instrumental PDSI being reconstructed [Cook *et al.*, 1999].

In developing our approach to reconstructing streamflow from the tree-ring based LBDA, we have capitalized on the fact that both variables are derivatives of a set of (unspecified) climate variables to which both streamflow and PDSI are sensitive (e.g., precipitation amount, temperature, and evaporation). Although variability is lost in each step of reconstructing PDSI from tree-rings and in reconstructing streamflow from the LBDA, it is possible that the reconstructed LBDA may remove noise irrelevant to hydrological variability rendering this paleoclimate reconstruction of PDSI particularly suitable for informing streamflow. Furthermore, streamflow and PDSI are inherently different hydrological variables as demonstrated in the temporal and spatial statistics shown in supporting information. Streamflow is also a derivative of a suite of nonclimatic variables such as catchment size, land-use, geology, topography, and groundwater interactions. These catchment-specific attributes are not explicitly considered in our study (with the exception of land use considered through the selection of streamflow gauges from relatively undisturbed catchments) and the inclusion of attributes could provide an improvement to the model [e.g., Thomas and Benson, 1970; Lima and Lall, 2010].

Assessments of hydrological variability on temporal scales broader than traditional hydrological practices are paramount to identifying long-term variations and quantifying the nature of persistent regimes, which are unachievable using comparatively short instrumental record. The understanding of paleoclimate variability facilitates the development of water and land use practices that are appropriate, sustainable, and resilient under previous patterns of hydroclimatic variability and complement efforts toward developing suitable adaptation procedures for projected future climate scenarios. While paleoclimate reconstructions of annual streamflow are useful for assessing long-term variability, annual information is often too coarse for water resource applications such as reservoir management and seasonal water allocations. In order to produce relevant data on a monthly or daily time step, a future undertaking could involve temporal disaggregation of the data. One method that could be utilized is a nonparametric k-nearest neighbors approach [Lall and Sharma, 1996; Rajagopalan and Lall, 1999; Nowak et al., 2010] that would avoid some issues associated with multisite stochastic generation schemes [Valencia and Schaake, 1973; Segond et al., 2006]. The objective of producing paleoclimate reconstructions of streamflow that are relevant for water resource management also suggests that the reconstruction of streamflow that is currently regulated would be valuable. Paleoclimate reconstructions of regulated streamflow could be achieved at an annual scale provided that regulations primarily impact the timing of subannual flows or if sufficient data prior to regularization exists. The resulting annual streamflow reconstruction could be disaggregated to a shorter timescale if preregulated flow data are available.

This study has capitalized on the availability of the spatially and temporally complete LBDA data set to attempt a reconstruction of streamflow on a broad spatial scale across the Missouri River Basin. The analysis employed here provides a feasible foundation from which streamflow reconstructions across the CONUS and North America could be implemented using the LBDA. In addition, the methodology presented here could be applied to reconstructing streamflow using other reconstructions of drought including the Monsoon Asia Drought Atlas [Cook et al., 2010b], the Old World Drought Atlas covering Europe, North Africa, and the Middle East [E. R. Cook et al., 2015] and the Australia and New Zealand summer drought atlas [Palmer et al., 2015].

Acknowledgments

We would like to sincerely thank Ben Cook (bc9z@ldeo.columbia.edu) for providing the LBDA data, the U.S. Geological Survey (USGS) for making their monthly streamflow data available (http://waterdata.usgs.gov/nwis/monthly?referred_module=sw), staff at the USGS (Christopher Ryan cmryan@usgs.gov and Thomas Weaver tlweaver@usgs.gov) for clarifying streamflow data availability; Siyan Wang for initial data collection; Scott Steinschneider, Xun Sun, and Pierre Gentine at the Columbia Water Center for their invaluable discussions on this work; and Juan A. Ballesteros and one other anonymous reviewer for their constructive comments.

Reconstruction results are available on the NOAA paleoclimate data base (<https://www.ncdc.noaa.gov/paleo/study/19520>). This work is funded by an NSF award 1360446 and NSF award 1401698. Lamont-Doherty contribution 8027.

References

- Allan, R. J. (2000), ENSO and climatic variability in the past 150 years, in *El Niño and the Southern Oscillation: Multiscale Variability and Global and Regional Impacts*, edited by Henry F. Diaz and Vera Markgraf, pp. 3–55, Cambridge Univ. Press, Cambridge, U. K.
- Allen, E. B., T. M. Rittenour, R. J. DeRose, M. F. Bekker, R. Kjelgren, and B. M. Buckley (2013), A tree-ring based reconstruction of Logan River streamflow, northern Utah, *Water Resour. Res.*, 49, 8579–8588, doi:10.1002/2013WR014273.
- Andreadis, K. M., E. A. Clark, A. W. Wood, A. F. Hamlet, and D. P. Lettenmaier (2005), Twentieth-century drought in the conterminous United States, *J. Hydrometeorol.*, 6(6), 985–1001, doi:10.1175/JHM450.1.
- Ault, T. R., J. E. Cole, J. T. Overpeck, G. T. Pederson, and D. M. Meko (2014), Assessing the risk of persistent drought using climate model simulations and paleoclimate data, *J. Clim.*, 27(20), 7529–7549, doi:10.1175/jcli-d-12-00282.1.
- Breshears, D. D., et al. (2005), Regional vegetation die-off in response to global-change-type drought, *Proc. Natl. Acad. Sci. U. S. A.*, 102(42), 15,144–15,148, doi:10.1073/pnas.0505734102.
- Brown, D. P., and A. C. Comrie (2004), A winter precipitation ‘dipole’ in the western United States associated with multidecadal ENSO variability, *Geophys. Res. Lett.*, 31, L09203, doi:10.1029/2003GL018726.
- Buuren, S. V., and K. Groothuis-Oudshoorn (2011), Mice: Multivariate imputation by chained equations in R, *J Stat. Software*, 45(3), 1–67, doi:10.18637/jss.v045.i03.
- Cole, J. E., J. T. Overpeck, and E. R. Cook (2002), Multiyear La Niña events and persistent drought in the contiguous United States, *Geophys. Res. Lett.*, 29(13), 1647, doi:10.1029/2001GL013561.

- Cook, B. I., R. L. Miller, and R. Seager (2009), Amplification of the North American "Dust Bowl" drought through human-induced land degradation, *Proc. Natl. Acad. Sci. U. S. A.*, 106(13), 4997–5001, doi:10.1073/pnas.0810200106.
- Cook, B. I., J. E. Smerdon, R. Seager, and E. R. Cook (2013), Pan-Continental droughts in North America over the last millennium, *J. Clim.*, 27(1), 383–397, doi:10.1175/jcli-d-13-00100.1.
- Cook, B. I., T. R. Ault, and J. E. Smerdon (2015), Unprecedented 21st century drought risk in the American Southwest and Central Plains, *Sci. Adv.*, 1(1), 1–7, doi:10.1126/sciadv.1400082.
- Cook, E. R., and P. J. Krusic (2004), *The North American Drought Atlas*, Lamont-Doherty Earth Observatory and National Science Foundation, N. Y.
- Cook, E. R., D. M. Meko, D. W. Stahle, and M. K. Cleaveland (1999), Drought reconstructions for the continental United States, *J. Clim.*, 12(4), 1145–1162, doi:10.1175/1520-0442(1999)012 < 1145:DRFTCU > 2.0.CO;2.
- Cook, E. R., K. R. Briffa, and P. D. Jones (1994), Spatial regression methods in dendroclimatology: A review and comparison of two techniques, *Int. J. Climatol.*, 14(4), 379–402, doi:10.1002/joc.3370140404.
- Cook, E. R., C. A. Woodhouse, C. M. Eakin, D. M. Meko, and D. W. Stahle (2004), Long-term aridity changes in the western United States, *Science*, 306(5698), 1015–1018, doi:10.1126/science.1102586.
- Cook, E. R., R. R. Seager, R. R. Heim, R. S. Vose, C. Herweijer, and C. Woodhouse (2010a), Megadroughts in North America: Placing IPCC projections of hydroclimatic change in a long-term palaeoclimate context, *J. Quat. Sci.*, 25(1), 48–61, doi:10.1002/jqs.1303.
- Cook, E. R., K. J. Anchukaitis, B. M. Buckley, R. D. D'Arrigo, G. C. Jacoby, and W. E. Wright (2010b), Asian monsoon failure and megadrought during the last millennium, *Science*, 328(5977), 486–489, doi:10.1126/science.1185188.
- Cook, E. R., J. G. Palmer, M. Ahmed, C. A. Woodhouse, P. Fenwick, M. U. Zafar, M. Wahab, and N. Khan (2013), Five centuries of Upper Indus River flow from tree rings, *J. Hydrol.*, 486, 365–375, doi:10.1016/j.jhydrol.2013.02.004.
- Cook, E. R., et al. (2015), Old World megadroughts and pluvials during the Common Era, *Sci. Adv.*, 1(10), 1–9, doi:10.1126/sciadv.1500561.
- Cutler, A., and L. Breiman (1994), Archetypal analysis, *Technometrics*, 36(4), 338–347, doi:10.1080/00401706.1994.10485840.
- Dai, A. (2013), Increasing drought under global warming in observations and models, *Nat. Clim. Change*, 3(1), 52–58, doi:10.1038/nclimate1633.
- De Bie, T., and B. De Moor (2003), On the regularization of canonical correlation analysis, in *International Symposium on ICA and BSS*, pp. 785–790, ICA2003, Nara, Japan.
- Dettinger, M. D., D. R. Cayan, H. F. Diaz, and D. M. Meko (1998), North–south precipitation patterns in western north America on interannual-to-decadal timescales, *J. Clim.*, 11(12), 3095–3111, doi:10.1175/1520-0442(1998)011 < 3095:NSPPIW > 2.0.CO;2.
- Devineni, N., U. Lall, N. Pederson, and E. Cook (2013), A tree-ring-based reconstruction of Delaware river basin streamflow using hierarchical Bayesian regression, *J. Clim.*, 26(12), 4357–4374, doi:10.1175/JCLI-D-11-00675.1.
- Dijkstra, T. (2014), Ridge regression and its degrees of freedom, *Qual. Quant.*, 48(6), 3185–3193, doi:10.1007/s11135-013-9949-7.
- Driscoll, D. (2013), *Hydroclimatic information and risk assessment methods for managing hydrologic extremes in the Missouri River Basin: A white paper for future studies*, Hydroclimatic extremes in the Missouri River Basin, U.S. Geol. Soc, United States.
- Fritts, H. C. (1976), *Tree Rings and Climate*, 567 pp., Academic.
- Galat, D. L., C. R. Berry Jr., E. J. Peters, and R. G. White (2005), Chapter 10: Missouri river basin, in *Rivers of North America*, edited by Arthur C. Benke and Colbert E. Cushing, pp. 426–480, Academic.
- Gallant, A. J. E., and J. Gergis (2011), An experimental streamflow reconstruction for the River Murray, Australia, 1783–1988, *Water Resour. Res.*, 47, W00G04, doi:10.1029/2010WR009832.
- Gedalof, Z. E., and D. J. Smith (2001), Interdecadal climate variability and regime-scale shifts in Pacific North America, *Geophys. Res. Lett.*, 28(8), 1515–1518, doi:10.1029/2000GL011779.
- Gershunov, A., and T. P. Barnett (1998), Interdecadal modulation of ENSO teleconnections, *Bull. Am. Meteorol. Soc.*, 79(12), 2715–2725, doi:10.1175/1520-0477(1998)079 < 2715:IMOET > 2.0.CO;2.
- González, I., S. Déjean, P. G. P. Martin, and A. Baccini (2008), CCA: An R package to extend canonical correlation analysis, 23(12), 1–14, doi:10.18637/jss.v023.i12.
- Herweijer, C., R. Seager, and E. R. Cook (2006), North American droughts of the mid to late nineteenth century: A history, simulation and implication for Mediaeval drought, *The Holocene*, 16(2), 159–171, doi:10.1191/0959683606hl917rp.
- Herweijer, C., R. Seager, E. R. Cook, and J. Emile-Geay (2007), North American droughts of the last millennium from a gridded network of tree-ring data, *J. Clim.*, 20(7), 1353–1376, doi:10.1175/JCLI4042.1.
- Higgins, R. W., Y. Yao, E. S. Yarosh, J. E. Janowiak, and K. C. Mo (1997), Influence of the great plains low-level jet on summertime precipitation and moisture transport over the Central United States, *J. Clim.*, 10(3), 481–507, doi:10.1175/1520-0442(1997)010 < 0481: IOTGPL > 2.0.CO;2.
- Ho, M., A. S. Kiem, and D. C. Verdon (2015), A paleoclimate rainfall reconstruction in the Murray-Darling Basin (MDB), Australia: 2. Assessing hydroclimatic risk using paleoclimate records of wet and dry epochs, *Water Resour. Res.*, 51, 8380–8396, doi:10.1002/2015WR017059.
- Ho, M., U. Lall, and E. R. Cook (2016), *Missouri River Basin 533 Year Annual Streamflow Reconstructions*, National Centers for Environmental Information, NESDIS, NOAA, U.S. Department of Commerce, Boulder, Colo. [Available <https://www.ncdc.noaa.gov/paleo/study/19520>.]
- Hornbeck, R. (2009), The enduring impact of the American dust bowl: Short and long-run adjustments to environmental catastrophe, *Natl. Bur. Econ. Res. Work. Pap. Ser.*, 15605, doi:10.3386/w15605.
- Hotelling, H. (1936), Relations between two sets of variates, *Biometrika*, 28(3–4), 321–377, doi:10.1093/biomet/28.3-4.321.
- Jolliffe, I. T. (2002), *Principal Component Analysis*, 2nd ed., 487 pp., Springer, N. Y.
- Jones, P. D., and M. E. Mann (2004), Climate over past millennia, *Rev. Geophys.*, 42, RG2002, doi:10.1029/2003RG000143.
- Kunkel, K. E., et al. (2013), Regional climate trends and scenarios for the U.S. National Climate Assessment. Part 4. Climate of the U.S. Great Plains, NOAA technical report no NESDIS 142-4, 82 pp., NOAA, Washington, D. C.
- Lall, U., and A. Sharma (1996), A nearest neighbor bootstrap for resampling hydrologic time series, *Water Resour. Res.*, 32(3), 679–693, doi:10.1029/95WR02966.
- Leurgans, S. E., R. A. Moyeed, and B. W. Silverman (1993), Canonical correlation analysis when the data are curves, *J. R. Stat. Soc. Ser. B*, 55(3), 725–740.
- Lima, C. H. R., and U. Lall (2010), Spatial scaling in a changing climate: A hierarchical Bayesian model for non-stationary multi-site annual maximum and monthly streamflow, *J. Hydrol.*, 383(3–4), 307–318, doi:10.1016/j.jhydrol.2009.12.045.
- Lockwood, J. G. (1999), Is potential evapotranspiration and its relationship with actual evapotranspiration sensitive to elevated atmospheric CO₂ levels?, *Clim. Change*, 41(2), 193–212, doi:10.1023/A:1005469416067.
- MacDonald, G. M., and R. A. Case (2005), Variations in the Pacific decadal oscillation over the past millennium, *Geophys. Res. Lett.*, 32, L08703, doi:10.1029/2005GL022478.

- Matalas, N. C., J. M. Landwehr, and M. G. Wolman (1982), Prediction in Water Management, in *Scientific Basis of Water Management*, pp. 118–122, edited by National Research Council (U.S.), Geophysics Study Committee, National Academy Press, Washington, D. C.
- McGowan, H. A., S. K. Marx, Denholm, J., Soderholm, and B. S. Kamber (2009), Reconstructing annual inflows to the headwater catchments of the Murray River, Australia, using the Pacific Decadal Oscillation, *Geophys. Res. Lett.*, 36, L06707, doi:10.1029/2008GL037049.
- Meko, D., C. W. Stockton, and W. R. Boggess (1995), The tree-ring record of sever sustained drought, *J. Am. Water Resour. Assoc.*, 31(5), 789–801, doi:10.1111/j.1752-1688.1995.tb03401.x.
- Monteith, J. (1965), Evaporation and environment, *Symp. Soc. Exp. Biol.*, 4, 1–4.
- Nohara, D., A. Kitoh, M. Hosaka, and T. Oki (2006), Impact of climate change on river discharge projected by multimodel ensemble, *J. Hydrometeorol.*, 7(5), 1076–1089, doi:10.1175/JHM531.1.
- Nowak, K., J. Prairie, B. Rajagopalan, and U. Lall (2010), A nonparametric stochastic approach for multisite disaggregation of annual to daily streamflow, *Water Resour. Res.*, 46, W08529, doi:10.1029/2009WR008530.
- Palmer, J. G., E. R. Cook, C. S. M. Turney, K. Allen, P. Fenwick, B. I. Cook, A. O'Donnell, J. Lough, P. Grierson, and P. Baker (2015), Drought variability in the eastern Australia and New Zealand summer drought atlas (ANZDA, CE 1500–2012) modulated by the Interdecadal Pacific Oscillation, *Environ. Res. Lett.*, 10(12), 124002, doi:10.1088/1748-9326/10/12/124002.
- Pederson, G. T. (2013), *Multi-century perspectives on current and future streamflow in the Missouri River Basin*, Northern Rocky Mountain Science Center, USGS. [Available at https://www.usgs.gov/centers/norock/science/multi-century-perspectives-current-and-future-streamflow-missouri-river-basin?qt-science_center_objects=1#qt-science_center_objects.]
- Pederson, N., A. R. Bell, E. R. Cook, U. Lall, N. Devineni, R. Seager, K. Eggleston, and K. P. Vranes (2012), Is an epic pluvial masking the water insecurity of the greater New York City region?, *J. Clim.*, 26(4), 1339–1354, doi:10.1175/JCLI-D-11-00723.1.
- Piechota, T. C., and J. A. Dracup (1996), Drought and regional hydrologic variation in the United States: Associations with the El Niño–Southern oscillation, *Water Resour. Res.*, 32(5), 1359–1373, doi:10.1029/96WR00353.
- Pizarro, G., and U. Lall (2002), El Niño-induced flooding in the U.S. West: What can we expect, *Eos Trans. AGU*, 82(32), 349–352, doi:10.1029/2002EO000255.
- Prairie, J., K. Nowak, B. Rajagopalan, U. Lall, and T. Fulp (2008), A stochastic nonparametric approach for streamflow generation combining observational and paleoreconstructed data, *Water Resour. Res.*, 44, W06423, doi:10.1029/2007WR006684.
- Quinn, W. H. (1992), A study of the Southern Oscillation-related climatic activity for A.D 622–1990 incorporating Nile River flood data, in *El Niño: Historical and Paleoclimatic Aspects of the Southern Ocean*, edited by Henry F. Diaz and Vera Markgraf, pp. 119–149, Cambridge Univ. Press, Cambridge.
- Rajagopalan, B., and U. Lall (1999), A k-nearest-neighbor simulator for daily precipitation and other weather variables, *Water Resour. Res.*, 35(10), 3089–3101, doi:10.1029/1999WR900028.
- Redmond, K. T., and R. W. Koch (1991), Surface climate and streamflow variability in the western United States and their relationship to large-scale circulation indices, *Water Resour. Res.*, 27(9), 2381–2399, doi:10.1029/91WR00690.
- Routson, C. C., C. A. Woodhouse, and J. T. Overpeck (2011), Second century megadrought in the Rio Grande headwaters, Colorado: How unusual was medieval drought?, *Geophys. Res. Lett.*, 38, L22703, doi:10.1029/2011GL050015.
- Seager, R., et al. (2007), Model projections of an imminent transition to a more arid climate in southwestern North America, *Science*, 316(5828), 1181–1184, doi:10.1126/science.1139601.
- Segond, M. L., C. Onof, and H. S. Wheater (2006), Spatial-temporal disaggregation of daily rainfall from a generalized linear model, *J. Hydrol.*, 331(3–4), 674–689, doi:10.1016/j.jhydrol.2006.06.019.
- Sheffield, J., E. F. Wood, and M. L. Roderick (2012), Little change in global drought over the past 60 years, *Nature*, 491(7424), 435–438, doi:10.1038/nature11575.
- Smerdon, J. E., B. I. Cook, E. R. Cook, and R. Seager (2015), Bridging past and future climate across paleoclimatic reconstructions, observations, and models: A hydroclimate case study, *J. Clim.*, 28(8), 3212–3231, doi:10.1175/JCLI-D-14-00417.1.
- Smith, S. R., P. M. Green, A. P. Leonardi, and J. J. O'Brien (1998), Role of multiple-level tropospheric circulations in forcing ENSO winter precipitation anomalies, *Mon. Weather Rev.*, 126(12), 3102–3116, doi:10.1175/1520-0493(1998)126<3102:ROMLTC>2.0.CO;2.
- Speer, J. H. (2010), *Fundamentals of Tree-Ring Research*, 333 pp., Univ. of Ariz. Press.
- St. George, S. (2010), Tree rings as paleoflood and paleostage indicators, in *Tree Rings and Natural Hazards: A State-of-Art*, edited by M. Stoffel et al., pp. 233–239, Springer, Netherlands.
- Steinschneider, S., and U. Lall (2015), Daily precipitation and tropical moisture exports across the eastern United States: An application of archetypal analysis to identify spatiotemporal structure, *J. Clim.*, 28(21), 8585–8602, doi:10.1175/JCLI-D-15-0340.1.
- Stone, E., and A. Cutler (1996), Introduction to archetypal analysis of spatiotemporal dynamics, *Phys. D*, 96(1–4), 110–131, doi:10.1016/0167-2789(96)00016-4.
- Thomas, D. M., and M. A. Benson (1970), Generalization of streamflow characteristics from drainage-basin characteristics, *U.S. Geol. Surv. Water Supply Pap.*, 1975, 55 pp.
- Thornthwaite, C. W. (1948), An approach toward a rational classification of climate, *Geogr. Rev.*, 38(1), 55–94, doi:10.2307/210739.
- Tierney, J. E., D. W. Oppo, Y. Rosenthal, J. M. Russell, and B. K. Linsley (2010), Coordinated hydrological regimes in the Indo-Pacific region during the past two millennia, *Paleoceanography*, 25, PA1102, doi:10.1029/2009PA001871.
- Tootle, G. A., and T. C. Piechota (2006), Relationships between Pacific and Atlantic ocean sea surface temperatures and U.S. streamflow variability, *Water Resour. Res.*, 42, W07411, doi:10.1029/2005WR004184.
- Torrence, C., and G. P. Compo (1998), A practical guide to wavelet analysis, *Bull. Am. Meteorol. Soc.*, 79(1), 61–78, doi:10.1175/1520-0477(1998)079<0061:APGTWA>2.0.CO;2.
- Trenberth, K. E., G. W. Branstator, and P. A. Arkin (1988), Origins of the 1988 North American Drought, *Science*, 242(4886), 1640–1645, doi:10.1126/science.242.4886.1640.
- U.S. Army Corps of Engineers (2006), *Missouri River Mainstem Reservoir System: Master Water Control Manual: Missouri River Basin*, 431 pp., Omaha, Nebraska.
- U. S. Geological Survey (2011), GAGES-II: Geospatial Attributes of Gages for Evaluating Streamflow, Va., US. [Available at http://water.usgs.gov/GIS/metadata/usgsrwd/XML/gagesII_Sept2011.xml, accessed 19 Jun.]
- Valencia, D., and J. C. Schaake (1973), Disaggregation processes in stochastic hydrology, *Water Resour. Res.*, 9(3), 580–585, doi:10.1029/WR009i003p00580.
- Vance, T. R., T. D. van Ommen, M. A. J. Curran, C. T. Plummer, and A. D. Moy (2013), A millennial proxy record of ENSO and eastern Australian rainfall from the law dome ice core, East Antarctica, *J. Clim.*, 26(3), 710–725, doi:10.1175/JCLI-D-12-00003.1.
- Vinod, H. D. (1976), Canonical ridge and econometrics of joint production, *J. Econom.*, 4(2), 147–166, doi:10.1016/0304-4076(76)90010-5.

- Vogel, R. M., U. Lall, X. Cai, B. Rajagopalan, P. Weiskel, R. P. Hooper, and N. C. Matalas (2015), Hydrology: The interdisciplinary science of water, *Water Resour. Res.*, 51, 4409–4430, doi:10.1002/2015WR017049.
- White, I. R., P. Royston, and A. M. Wood (2011), Multiple imputation using chained equations: Issues and guidance for practice, *Stat. Med.*, 30(4), 377–399, doi:10.1002/sim.4067.
- Wilson, R., E. Cook, R. D'Arrigo, N. Riedwyl, M. N. Evans, A. Tudhope, and R. Allan (2010), Reconstructing ENSO: The influence of method, proxy data, climate forcing and teleconnections, *J. Quat. Sci.*, 25(1), 62–78, doi:10.1002/jqs.1297.
- Wise, E. K. (2010), Spatiotemporal variability of the precipitation dipole transition zone in the western United States, *Geophys. Res. Lett.*, 37, L07706, doi:10.1029/2009GL042193.
- Woodhouse, C. A., and D. Meko (1997), Number of winter precipitation days reconstructed from southwestern tree rings, *J. Clim.*, 10(10), 2663–2669, doi:10.1175/1520-0442(1997)010<2663:NOWPDR>2.0.CO;2.
- Woodhouse, C. A., and J. T. Overpeck (1998), 2000 years of drought variability in the central United States, *Bull. Am. Meteorol. Soc.*, 79(12), 2693–2714, doi:10.1175/1520-0477(1998)079<2693:YODVIT>2.0.CO;2.
- Woodhouse, C. A., J. Lukas, B. Brice, K. Hirschboeck, H. Hartmann, M. Kostuk, E. Lay, D. Martinex, B. McMahan, and A. Shah (2002), Tree Rings and Streamflow. [Available at <http://treeflow.info/content/tree-rings-and-streamflow>, 1 June 2015.]
- Woodhouse, C. A., K. E. Kunkel, D. R. Easterling, and E. R. Cook (2005), The twentieth-century pluvial in the western United States, *Geophys. Res. Lett.*, 32, L07701, doi:10.1029/2005GL022413.
- Woodhouse, C. A., S. T. Gray, and D. M. Meko (2006), Updated streamflow reconstructions for the Upper Colorado River Basin, *Water Resour. Res.*, 42, W05415, doi:10.1029/2005WR004455.
- Woodhouse, C. A., D. M. Meko, G. M. MacDonald, D. W. Stahle, and E. R. Cook (2010), A 1,200-year perspective of 21st century drought in southwestern North America, *Proc. Natl. Acad. Sci. U. S. A.*, 107(50), 21,283–21,288, doi:10.1073/pnas.0911197107.